C. R. Chimie 5 (2002) 815–824

S1631074802014492/REV

Rare-earth-doped glasses for fiber amplifiers in broadband telecommunication

Setsuhisa Tanabe*

Faculty of Integrated Studies, Kyoto University, Kyoto 606-8501, Japan

Received 30 April 2002; accepted 28 May 2002

Abstract – Rare-earth-doped optical amplifiers have a great potential for broadband Wavelength-Division-Multiplexed (WDM) telecommunication by tailoring host glass compositions. In order to design the emission spectra of doped rare-earth ions, it is important to understand the relationship between the local ligand field and various optical properties of specific 4f-levels, such as the radiative transition probability, the nonradiative decay probability, which dominate the spectral line width and quantum efficiency of amplification transitions. For the Er^{3+}:1.55 μm transition, the role of the Judd–Ofelt Ω_6 parameters is presented, which is correlated to the Er–ligand bond covalency in glasses. The Tm^{3+}: 1.46-μm transition shows quantum efficiency over 90% high enough for the S-band application, in heavy metal oxide glasses with moderate phonon energy and wider spectra than fluorides. A way to improve population inversion by selective energy transfer with codoped lanthanide ions is presented. Finally, the energy level structures and resultant spectral properties of Pr^{3+}, Nd^{3+} and Dy^{3+} ions, 1.3-μm-active ions, are compared. The hypersensitivity of Dy^{3+} transitions appears especially in chalcogenide glasses, where the nonradiative loss due to multiphonon decay is also minimized. In conclusion, glass materials have opportunities to vary the radiative cross section, quantum efficiency, and gain flatness, which are important for novel amplifiers in the future DWDM system. ***To cite this article: S. Tanabe, C. R. Chimie 5 (2002) 815–824*** © 2002 Académie des sciences / Éditions scientifiques et médicales Elsevier SAS

rare earths / glass / optical amplifier / telecommunication / Wavelength-Division Multiplexing / optical fiber

Résumé – Les télécommunications à large bande basées sur le multiplexage en division de longueur d'onde (WDM) font appel à des amplificateurs optiques dopés avec des terres rares. Le spectre d'émission de ces terres rares peut être ajusté en modifiant la composition du verre. Il faut pour cela connaître la relation entre le champ local et les caractéristiques optiques des niveaux concernés, en particulier les probabilités de transition radiative et de désexcitation non radiative, qui déterminent la largeur spectrale et le rendement quantique des transitions. Le rôle du paramètre de Judd–Ofeld Ω_6 dans la transition de l'erbium à 1,55 μm est corrélé à la covalence de la liaison Er–ligande dans le verre. Les transitions du Tm^{3+} pour la bande S et celle des ions Pr^{3+}, Nd^{3+} et Dy^{3+} à 1,3 μm sont également abordées et discutées. Dans les matériaux vitreux, on peut ainsi faire varier la section efficace radiative, le rendement quantique et la constance du gain, ce qui peut se révéler important pour les nouveaux amplificateurs dans les futurs systèmes DWDM. ***Pour citer cet article : S. Tanabe, C. R. Chimie 5 (2002) 815–824*** © 2002 Académie des sciences / Éditions scientifiques et médicales Elsevier SAS

terres rares / verre / amplificateur optique / télécommunication / *Wavelength-Division Multiplexing* (WDM) / fibre optique

1. Introduction

The growing demand and future potentials of an advanced information society stimulate research for devices composing a network system with excellent flexibility and larger information capacities at much faster rates. Installation of broadband Wavelength-Division-Multiplexing (WDM) optical network system is indispensable and novel amplifier materials, which would overcome the performance of the present silica-based erbium-doped fiber amplifier (EDFA), can be a key to enable more number of channels. Among several possible choices of devices, rare-earth-doped amplifiers have implied high-power conversion effi-

* *Correspondence and reprints.*
E-mail address: stanabe@gls.mbox.media.kyoto-u.ac.jp (S. Tanabe).

ciency than Raman and scalability of gain spectra by tailoring the host-glass composition. In telecommunication systems, the invention of the EDFA [1] can be likened to that of the transistors in electronics in terms of its technological impact. The technology to amplify the light signal directly without the conversion of light/electricity/light has been achieved by stimulated emission of 4f optical transition in rare-earth-doped fibers [2], which realizes ideal amplification with high gain and low noise. The technological development of optical telecommunication is based on the growth of technologies of fiber fabrication and those of laser diodes (LD). In fact, the invention of efficient III-V LD has also enabled efficient pumping of Er^{3+} with its three-level system [3–5]. In addition, there exists the history of technological transition from passive fibers to active fibers [2], in which we can find a quite interesting relationship between active ions and the host glasses. Although the fiber amplifiers are already playing crucial roles in the optical networks both at 1.55 μm and at 1.3 μm bands, there exist further requirements to fully utilize the window of optical fibers with superior performance. The requirements are wide and flat gain spectrum around 1.53~1.65 μm (C+L band) in a novel EDFA and around 1.45~1.51 μm (S-band) in Tm^{3+} (TDFA) for the WDM systems [6], greater gain per pump-power at 1.31 μm in Pr^{3+}- [7, 8] or possibly Dy^{3+}-doped glasses [9–11].

According to the report of the Japanese Photonic Network Research Committee, the DWDM system will require 3000 channels in the year 2010 [12]. To enable 3000-channel WDM, we need more various amplifiers as well as a transmission fiber with a window from 1 to 1.65 μm. Fig. 1 shows a typical loss spectrum of the present silica fiber and emission bands of several rare-earth ions.

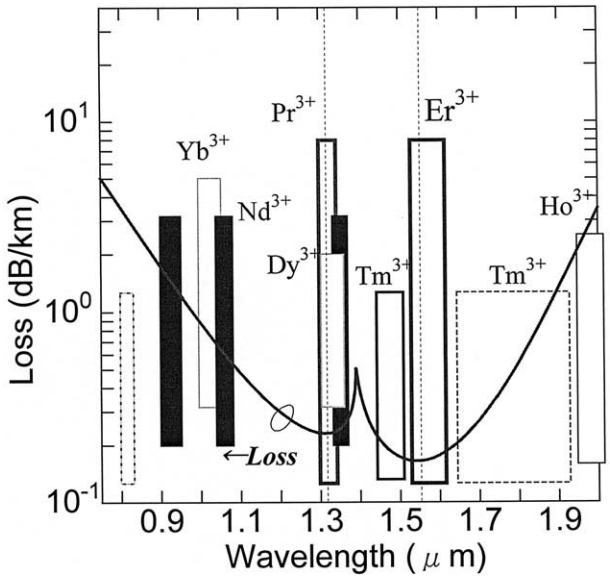

Fig. 1. Loss characteristics of silica fiber and emission bands of some rare-earth ions.

Not only in fiber forms, planar waveguide forms will also play a role in photonic devices, since integration of optical circuits improves functions with fewer components [13]. Because a shorter device length is usually expected for these waveguides, it might suffer from the problem of concentration quenching and new solutions of host materials would be required, due to the need of greater doping concentrations of rare-earth ions. In devices of either form, it is necessary to understand the 4f transitions of the ions, the structure of their sites in glass to design amplifier materials with better properties. This paper reviews some studies on the spectroscopic properties, radiative and nonradiative processes, and site structure of rare-earth ions in glasses at each wavelength.

2. Research scheme for rare-earth laser glasses

An optical amplifier works by the principle of light amplification by stimulated emission of radiation, nothing different from that of lasers. It requires a pump to create a population inversion in the amplifier medium. When an incoming signal photon stimulates an excited electron, the electron relaxes back into a lower energy state and emits a second signal photon with the same phase as the incoming photon. This process of stimulated emission amplifiers the signal. The success of the first generation silica-based EDFA is that the energy level of Er^{3+} ions can cause amplification to emit a photon with precisely the wavelength at which the network operates, with high efficiency, even in silica hosts having high phonon energy and poor RE solubility. The erbium was really a lucky boy to be the first, with an ideal energy level structure workable in silica and several pumping LDs available. Anyway, it is not a surprising idea to apply a research scheme for various rare-earth laser glasses to the design of novel amplifiers. To quantitatively comprehend optical phenomena of rare-earth ions in glasses, it is important to evaluate radiative and nonradiative decay process of related 4f levels. The Judd-Ofelt theory is usually adopted to obtain the radiative transition probabilities including emission by utilizing the data of absorption cross-sections of several f–f electric-dipole lines, especially for four-level emissions. The physical and chemical implement of three Ω_t parameters ($t = 2,4,6$) are becoming clearer by combining the information of the local ligand field of doped ions by other spectroscopic techniques such as the ^{151}Eu-Mössbauer effect [14]. In some cases, the isomer shift and quadrupole splitting give us more discrete information about the rare-earth environment

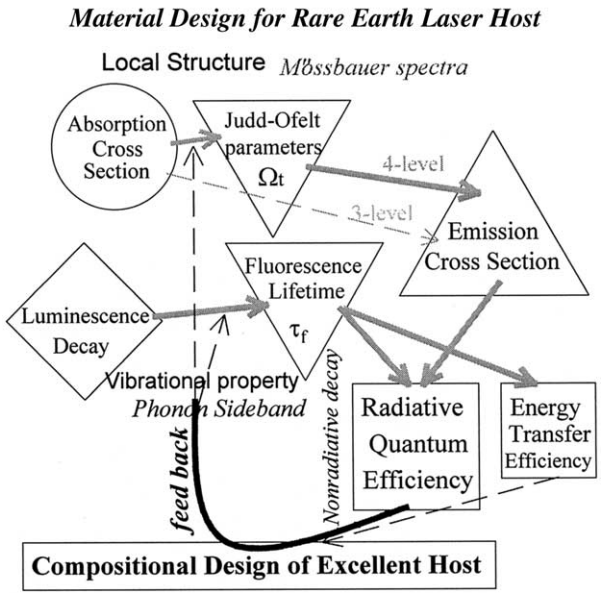

Fig. 2. Research scheme for efficient laser materials.

in glass; bond covalency and symmetry [15]. The nonradiative decay rate can be evaluated experimentally by combining the lifetime measurement, which include contributions of multiphonon decay, energy transfer such as cross relaxation, cooperative upconversion, etc. In order to distinguish each contribution, systematic studies on concentration dependence of the rates are necessary. The phonon sideband spectra of Eu^{3+} ion can be supplementary to inclusive understanding of local structure in glass hosts, where the stretching vibrational mode of the network former bond often plays an important role [16] in the decay as well as in the phonon-assisted energy transfer [17]. The above-mentioned research scheme is shown in Fig. 2. In many cases, the site selectivity of doped RE ions cannot be predicted in multicomponent glasses. However, we can feed back the several characteristics obtained for selected glasses toward a better material design based on logical direction.

3. The 1.55-μm band in Er^{3+}-doped glasses for broadband amplifiers

There is now a worldwide consensus that the WDM networking has superior functions and applications for future telecommunication systems [18] to the single channel TDM only at 1.55 μm. It offers not only large-scale information capacity, but also flexibility and transparency by utilizing the properties of light. Among various properties of EDFA, such as low-noise, broad bandwidth (not broad enough now!!) and efficient gain, the ability to amplify more than one wavelength at a time has replaced the regenerator for each channel. Although the excellent performance of the present silica-based EDFA can be used for a WDM system, but with fewer channels, there exists requirement for a larger number of channels, which could be possible by using an EDFA with a wider gain spectrum [6]. From a practical standpoint, the flatness of the gain is also critically important because the light intensity for different channels would be varied by the multi-step amplifications if the gain of the amplifier were not independent of wavelengths. Therefore, the design of a host for Er^{3+} for wide and flat spectra of the $^4I_{13/2}$–$^4I_{15/2}$ transition at around 1.5~1.6 μm is a target at present.

For the transitions between the states with the difference in the total angular momentum by $\Delta J = 1$, there exists the contribution of the magnetic-dipole transition [19] in the $^4I_{13/2}$–$^4I_{15/2}$. The spontaneous emission probability of this transition is given by:

$$A_{J'J} = \frac{64\,\pi^4\,e^2}{3\,h(2\,J'+1)\,\lambda^3}\left\{\left[\frac{n(n^2+2)^2}{9}\right]\times S^{\mathrm{ed}} + n^3 \times S^{\mathrm{md}}\right\} \quad (1)$$

where h is the Planck constant, m and e are the mass and charge of the electron, c is the velocity of light, n is the refractive index at the mean wavelength, λ, S^{ed} and S^{md} are the line strengths of the electric-dipole and magnetic-dipole transitions, respectively. The S^{md} is characteristic of the transition and thus a constant. Thus the second term is not varied with ligand field and dominated only by the refractive index, which has usually about 30% contribution in silicate glasses. That is part of the reason why the Er^{3+} ions in silicate glasses have a narrow 1.55 m spectrum [20]. In order to get flat emission spectra, it can be effective to increase the relative contribution of the electric-dipole transition, the spectra of which can be varied due to the variations of width of the Stark splitting ($J + 1/2$), inhomogeneous broadening in amorphous structures and also to sensitivity to the local fields [21–23]. While the line strength of the magnetic-dipole transition is independent of ligand fields, whereas that of the electric-dipole transition is a function of them [20, 21]. According to the Judd–Ofelt theory [24, 25], the line strength of the electric dipole components of the 1.55-μm transition is given by [26]:

$$S^{\mathrm{ed}}[^4I_{13/2};^4I_{15/2}] = \sum_{t=2,4,6} \Omega_t < {}^4I_{13/2}\|U^{(t)}\|{}^4I_{15/2} >^2$$
$$= 0.019\,\Omega_2 + 0.118\,\Omega_4 + 1.462\,\Omega_6 \quad (2)$$

where the three coefficients of Ω_t are the reduced matrix elements of the unit tensor operators, $U^{(t)}$, calculated in the intermediate-coupling approximation, and Ω_t ($t = 2,4,6$), are the intensity parameters. Since the <SLJ $|U^{(t)}|$ S'L'J'> of other transitions are also a constant characteristic of each transition, three inten-

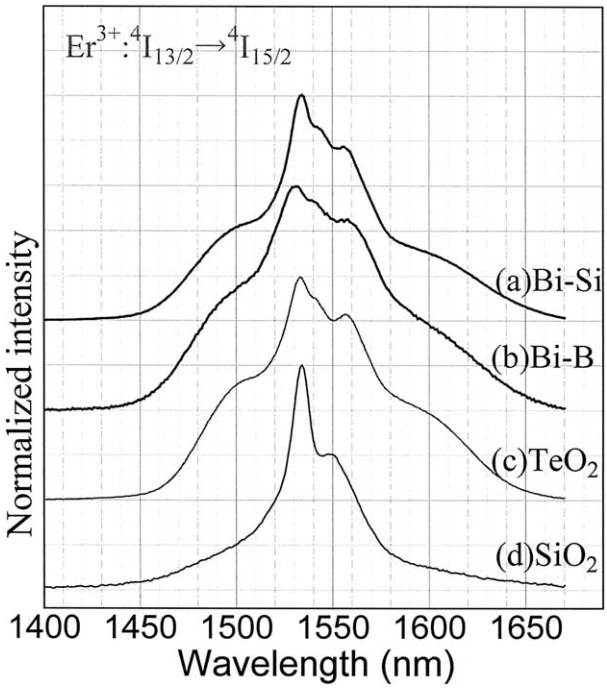

Fig. 3. Fluorescence spectra of Er^{3+}-doped glasses; (**a**) Bi-silicate, (**b**) Bi-borate, (**c**) Tellurite and (**d**) Al-silica.

sity parameters Ω_t (t = 2,4,6) can be obtained from more than three measured absorption cross-sections by using the method of least squares fitting [27]. What varies depending on the host composition and structures is the electric-dipole transitions, where the Ω_6 parameter is dominant. Excellent spectra with larger cross-section are observed in tellurite [6] and bismuth-based oxide glasses [28] (Fig. 3), than aluminosilicates [20]. The higher bond-ionicity is confirmed for the glasses with a large Ω_6 of Er^{3+} by ^{151}Eu Mössbauer spectroscopy, which can be explained by the largest contribution of the overlap integral of 4f and 5d orbitals [14, 21]. Also there may be another possible reason. The relative ratio of the field correction factors $(n^2 + 2)^2/9\,n^2$ takes a minimum at $n = 1.414$ and increases monotonically with increasing n; i.e., under constant S^{ed} and S^{md}, the relative contribution of ED transition should increase with increasing n of the host glass, which is not practically the case, because these values are not independent. However, it is empirically true that many glass hosts with a large n show broad Er^{3+} emission spectra. There are few exceptions from the tendency that the Er^{3+} ions in those glasses take a large Ω_6 value, since the electron polarizability and bond covalency are strongly correlated.

4. Tm-doped glasses for S-band amplifier

4.1. Background of S-band requirement

Due to the rapid increase of information traffic, great research effort has been paid to development of telecommunication devices for the WDM network system [29]. Because the silica-based transmission fiber has a wide and low-loss window from 1.4 to 1.65 μm, there is an emergent demand for optical amplifiers, which can be used around 1.4 and 1.6 μm, in addition to the present silica-based EDFA. Tellurite-based EDFA was reported to have 80-nm-wide gain up to 1.6 μm (L-band), which also shows various excellent material properties [30, 31]. For the 1.45–1.49-μm band (S^+-band), the fluoride-based Tm-doped fiber (TDF) [32] can be used as an amplifier, although it still presents difficulties compared with the use of EDFA. One of the reasons for inferior performance of TDFA is a longer lifetime of the terminal $^3F_4$ level than that of the initial $^3H_4$ level [33]. The performance of the TDFA is improved by use of an upconversion pumping scheme with a 1.06-μm laser, which produces a population inversion. Codoping of other lanthanide ion, such as Ho^{3+}, was also found to improve the population inversion by means of the energy transfer from the $^3F_4$ level [34]. In addition, a larger branching ratio, β of the $^3H_4 \rightarrow {}^3H_6$ band at 0.80 μm than that of the 1.46 μm make it difficult to realize amplification, because the fiber can easily lase at 0.80 μm, resulting in the gain saturation [35]. According to the Judd–Ofelt calculation, β of 0.80 μm is nearly 90%, which is 11 times larger than that of 1.46 μm emission in most glasses [36, 37]. Therefore, the suppression of the 0.80 μm amplified spontaneous emission (ASE) is desirable to avoid lasing at unexpected wavelength for improving the amplifier performance. In either case, in spite of difficulty as practical materials, nonoxide-fiber hosts with lower phonon energy have been used, because the $^3H_4$ level is more easily quenched in high-phonon-energy environment, due to its small energy gap. However, the energy gap of the $^3H_4$ level is not so small as that of the Pr:$^1G_4$ for 1.3-μm amplifiers and thus good performance can be expected in some oxide hosts with low phonon energy and better fiberizability.

Fig. 4 shows the relation between the multiphonon decay rate, W_p of the Tm:$^3H_4$, Pr:$^1G_4$ levels and the inverse phonon energy of various glass hosts. We can see the lower W_p of the Tm:$^3H_4$ in tellurite than that of the Pr:$^1G_4$ in ZBLAN, even with higher phonon energy.

In this chapter, the tellurite glass was chosen as a host because it has relatively low phonon energy, excellent properties for fiber fabrications [30, 38], and thus can be considered as a candidate material for TDFA.

4.2. Spectroscopy of singly doped glass

4.2.1. Fluorescence spectra

Fig. 5 shows the Tm^{3+} energy level and a fluorescence spectrum in the tellurite glass, excited at

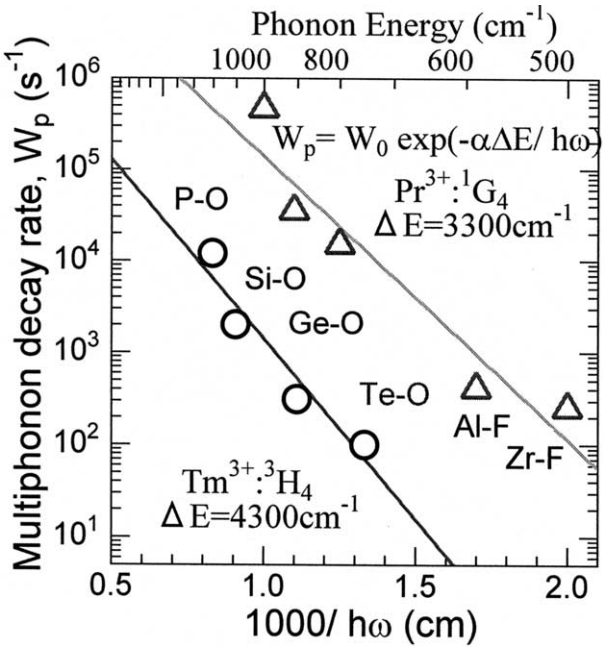

Fig. 4. Relationship between multiphonon decay rates of Tm^{3+}:$^3H_4$, Pr^{3+}:$^1G_4$ levels and inverse phonon energy.

790 nm. The emission bands at 0.80 μm, 1.46 μm, and 1.80 μm are due to the $^3H_4 \rightarrow {}^3H_6$, $^3H_4 \rightarrow {}^3F_4$, and $^3F_4 \rightarrow {}^3H_6$ transitions, respectively. The wavelength region longer than 1.3 μm is multiplied by 10 times. The area integration was carried out after converting the wavelength into wavenumber scale, which is directly proportional to the energy. The relative intensity ratio of 0.80 to 1.46 μm was about 11, almost unchanged with glass compositions and Tm-concentration. On the other hand, that of 1.46 to 1.80 μm was largely changed with these factors, which is due to the effect of the nonradiative relaxations.

Table 1. Spontaneous emission probability and branching ratios of Tm^{3+}:$^3H_4$ level in the tellurite glass.

Transition	A^{ed} (s^{-1})	A^{md} (s^{-1})	Calculated branch ratio β(%)	Ratio of measured emission band
$^3H_4 \rightarrow {}^3H_6$	2426	–	88.8	~11
$^3H_4 \rightarrow {}^3F_4$	229	–	8.4	1
$^3H_4 \rightarrow {}^3H_5$	54	23	2.8	–
	$A_{total} = 2732\ s^{-1}$, $\tau_{rad} = A^{-1} = 366$ s			

4.2.2. Judd–Ofelt analysis and quantum efficiency in tellurite

The obtained Judd–Ofelt parameters of Tm^{3+} in the present glass were: $\Omega_2 = 4.69\ pm^2$, $\Omega_4 = 1.83\ pm^2$, $\Omega_6 = 1.14\ pm^2$. Table 1 shows spontaneous emission probabilities, A and β from the $^3H_4$ level of Tm^{3+} ions in the tellurite glass. The β of 0.80-μm emission is 11 times larger than that of 1.4-μm emission, which is almost similar to the case in fluoride and other oxide glasses. The calculated τ_R was 366 μs, while the measured lifetime was 350 μs. This indicates that the quantum efficiency of the $^3H_4$ level is 96% in tellurite glass, which is comparable to that in ZrF_4-based fluoride glasses (~100%).

4.2.3. Concentration dependence of emission

Fig. 6 shows the Tm_2O_3-concentration dependence of ratios of the $\tau_f(^3F_4)/\tau_f(^3H_4)$ and the integrated intensity of (1.80 μm)/(1.46 μm) of fluorescence spectra. Both

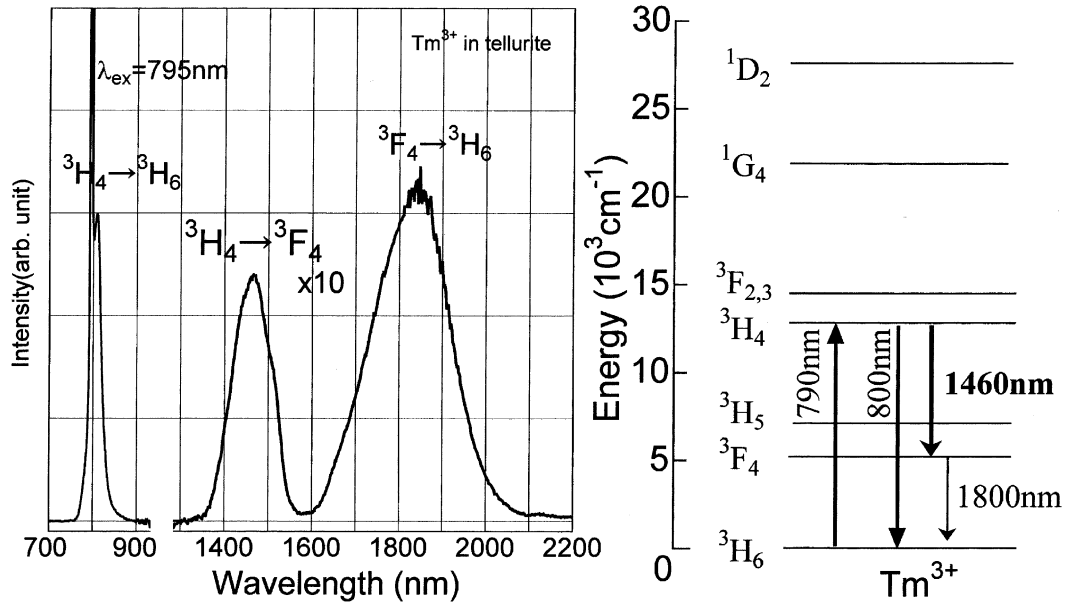

Fig. 5. Fluorescence spectra of Tm^{3+}-doped tellurite glass. Energy level of Tm^{3+} ion is also shown for assignment.

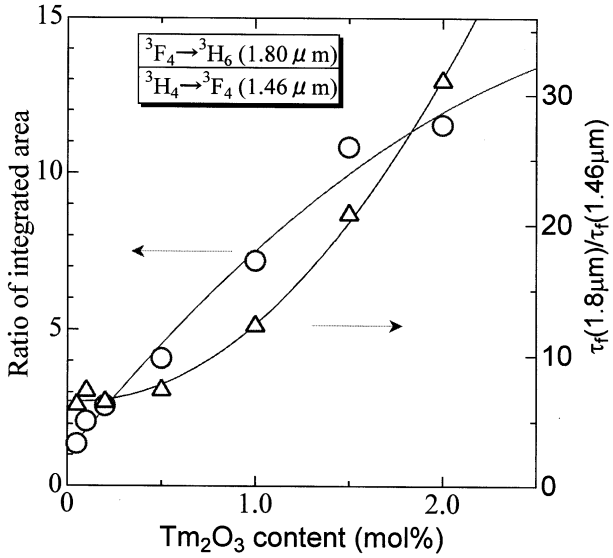

Fig. 6. Ratio of integrated area and lifetime of 1.4 μm/1.8 μm in 72 TeO_2–20 ZnO–5 Na_2O–(2.9 – x) Y_2O_3–x Tm_2O_3 glasses.

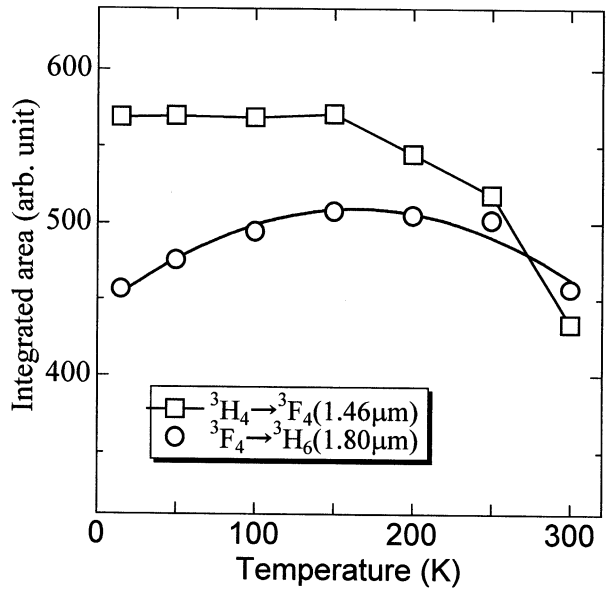

Fig. 8. Temperature dependence of the integrated area of the 1.4-μm and 1.8-μm band in the 0.1 Tm_2O_3 glass.

ratios increase drastically with increasing the Tm_2O_3 content. These phenomena are well understood by the so-called 'Two-for-One Process' [31], which is a result of the cross relaxation between two Tm^{3+} ions; $[^3H_4,{}^3H_6] \rightarrow [^3F_4,{}^3F_4]$ and unfavorable for population inversion between the $^3H_4$ and $^3F_4$ levels. Therefore, a low concentration is desirable to keep a high quantum efficiency of the $^3H_4$ level for 1.4-μm application.

4.2.4. Temperature dependence

Fig. 7 shows temperature variation of the fluorescence spectra. The peak intensity of the 1.46-μm band increases with lowering temperature, while the line shape of the 1.8-μm band becomes sharp. It can be seen that the mean wavelength of both bands shift to the longer side. The temperature dependence of integrated intensities of both bands is plotted in Fig. 8. The integrated area of the 1.46-μm band is almost unchanged at lower temperature and drops with temperature above 150 K. On the other hand, that of the 1.8-μm band increases slightly and decreases above 250 K. The tendency of the 1.46-μm emission can be explained by considering the temperature dependence of the nonradiative decay from the $^3H_4$ level, which has smaller energy gap to the next lower level. The increasing tendency of the 1.8-μm band is ascribed to the improved population from the upper level by nonradiative processes. Therefore, the lower the temperature is, the better the population inversion becomes. Another advantage of the lower temperature can be the much-improved intensity at 1.50–1.52 μm, which is hardly obtained by conventional EDFA, though not impossible by TDFA [39].

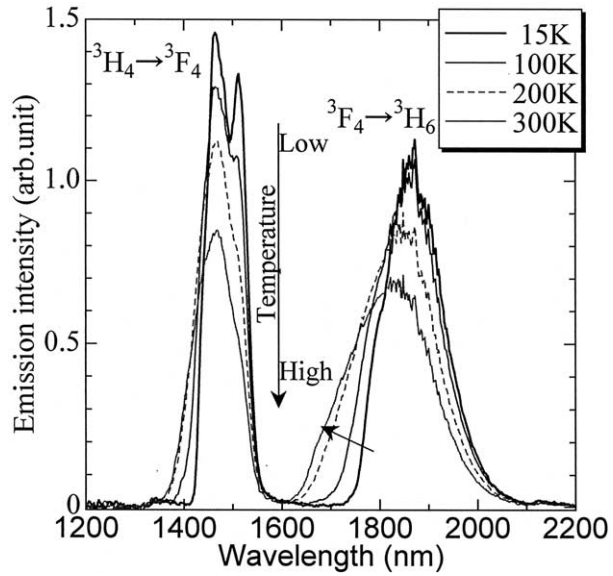

Fig. 7. Temperature dependence of fluorescence spectra of 72 TeO_2–20 ZnO–5 Na_2O–2.9 Y_2O_3–0.1 Tm_2O_3 glass.

4.3. Effect of codoping of Ho, Tb, Eu

One of the possibilities to improve the population inversion can be a selective quenching of the terminal level by codoping of other lanthanide [34, 40], because nothing is better than to pump directly the $^3H_4$ with 0.79-μm LD of AlGaAs rather than upconversion scheme [35, 41]. The role expected for a codopant is to quench the $^3F_4$ level selectively without quenching the $^3H_4$ level. From this viewpoint, the Eu^{3+}, Tb^{3+} and Ho^{3+} can be a candidate among 13 4f-active lanthanide

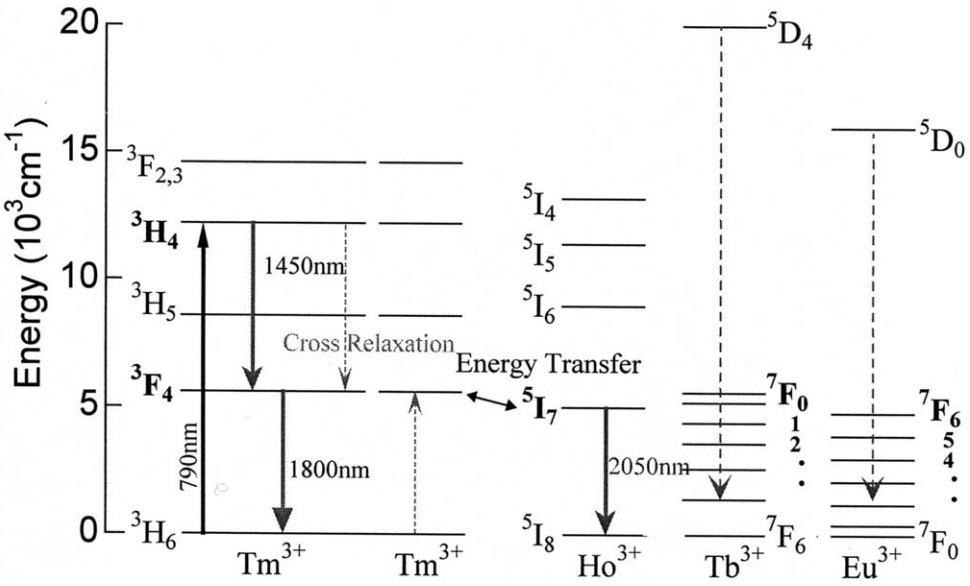

Fig. 9. Energy level of Tm^{3+}, Ho^{3+}, Tb^{3+} and Eu^{3+} ion.

ions. The energy level diagrams of these ions are shown in Fig. 9. The *Ln*-concentration dependence of the lifetimes of the Tm^{3+}:$^3H_4$ and $^3F_4$ levels is plotted in Fig. 10. Among three codopants, the Eu^{3+} ion quenches both levels most significantly and the Ho^{3+} ion shows the best selectivity; i.e., the least effect on the $^3H_4$ lifetime with a large quenching effect on the $^3F_4$. The variation of the fluorescence spectra of Tm–Ho codoped tellurite glasses are shown in Fig. 11. The spectra are normalized by the intensity of 1.46-μm band, because it showed the least change. We see a drastic decrease of the 1.8-μm band and a rapid increase of the Ho^{3+}:$^5I_7 \rightarrow {}^5I_8$ emission intensity at 2 μm. This result is an evidence of the Tm:$^3F_4 \rightarrow$ Ho:$^5I_7$ energy transfer.

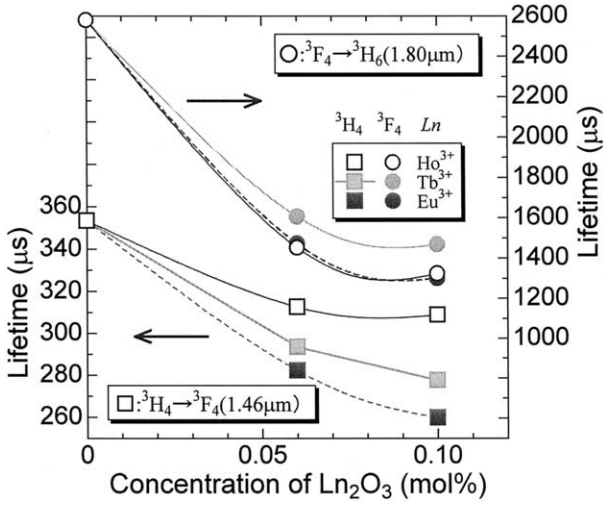

Fig. 10. Effect of codopant on the lifetime of Tm^{3+} levels.

5. Active ions at 1.3 μm

5.1. Comparison of candidates

The world land-based optical networks installed are composed of 1.3 μm zero-dispersion silica fiber. However, no practical amplifiers have sufficient performance at 1.3-μm like EDFAs at 1.55-μm band. Fig. 12 shows the energy levels of Pr^{3+}, Nd^{3+}, and Dy^{3+} ions, which are active ions at 1.3 μm. Based on the huge amount of data on laser glasses for 1.06-μm applications [42], the Nd^{3+} ion was extensively studied as a candidate at first

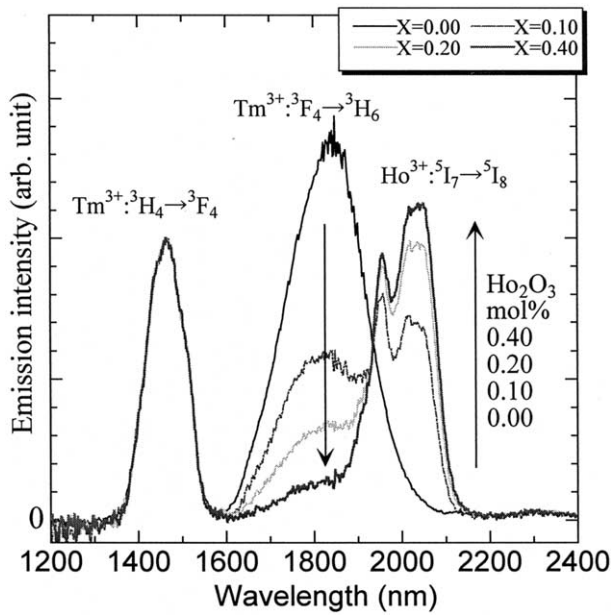

Fig. 11. Fluorescence spectra of 72 TeO_2–20 ZnO–5 Na_2O–(2.9 – *x*) Y_2O_3–*x* Ho_2O_3–0.1 Tm_2O_3 glasses.

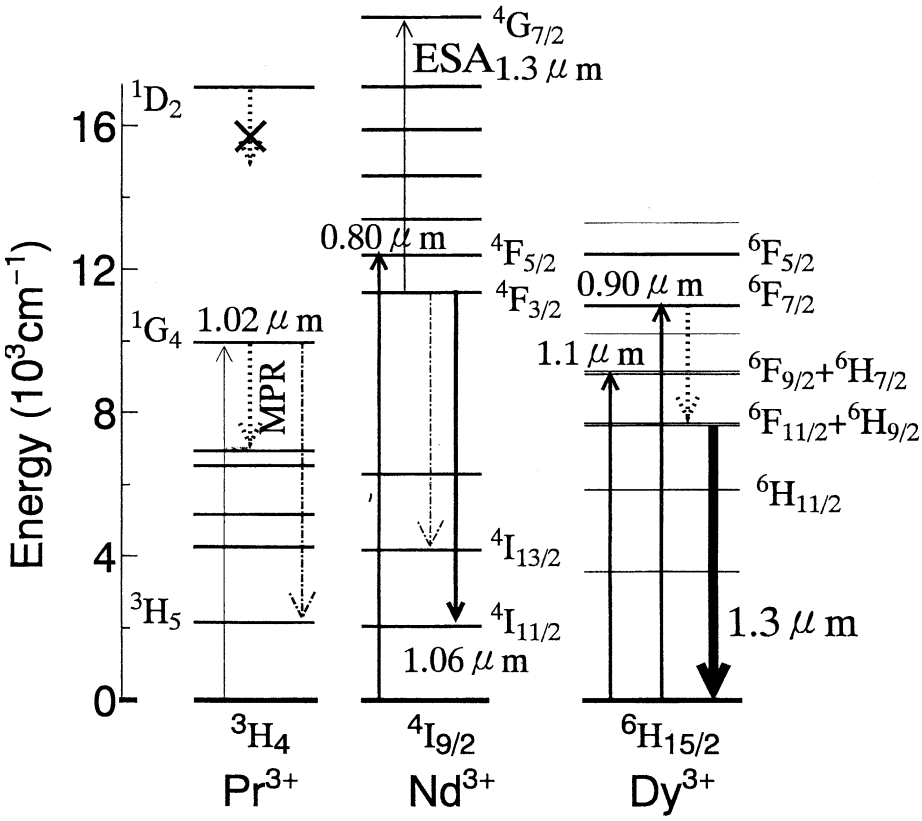

Fig. 12. Energy level of Pr^{3+}, Nd^{3+} and Dy^{3+} ion.

in many glasses. However, the excited state absorption from the $^4F_{3/2}$ and the resulting gain shift to 1.35 μm were found to be a problem as well as a small branching ratio compared with that of 1.06 μm, which is a cause of intense amplified spontaneous emission (ASE) [43]. The Pr^{3+} ion is probably most often studied in fluoride [7] and chalcogenide glasses [8] and practical devices have already been produced [44]. The branching ratio from the $^1G_4$ level is usually more than 60% in most glasses [45]. The nonradiative loss due to the small energy gap limits the choice of host to nonoxide glasses. In addition, the small absorption cross-section of the only pumpable level ($^1G_4$) at 1.02 μm must be overcome by high-power pumping laser. Nonradiative population from the upper $^1D_2$ level cannot be expected due to its larger energy gap. Since it is difficult to get high-quality lasers at 1.02 μm with semiconductor lasers, an 0.8 μm-LD- pumped Nd:$YLiF_4$ solid-state laser (λ = 1047 nm) is often used as a pumping source [45]. Among various glasses, the Ga–Na–S system has the highest quantum efficiency of 62% and the largest gain per pumping power at 1.34 μm [8]. However, the gain at 1.31 μm is still low partly due to the peak shift to longer wavelength in sulfides [8].

Compared with these two ions, the Dy^{3+} has unique properties, though it is also affected by multiphonon loss. The Dy^{3+} ion can be pumped by 0.8 μm, 0.9 μm, 1.1 μm or 1.28 μm with large cross sections, for which the high-power LD's can be used. Table 2 shows the reduced matrix elements of 1.3-μm emission transitions for Pr^{3+}, Nd^{3+} and Dy^{3+} ions [11]. While the transition probabilities in Pr^{3+} and Nd^{3+} ions depend most largely on Ω_6, that in Dy^{3+} is dominated by the Ω_2 parameter, which is most sensitive to the local symmetry and thus to the glass composition. The transition, the cross section of which is very sensitive to the local structure, is called '*hypersensi-*

Table 2. Reduced matrix elements of 1.3-μm emission transitions for Pr^{3+}, Nd^{3+} and Dy^{3+} ions [11].

Ln^{3+}	$4f^N$	aJ	bJ'	$<U^{(2)}>^2$	$<U^{(4)}>^2$	$<U^{(6)}>^2$	λ (μm)
Pr^{3+}	2	$^1G_4$	$^3H_5$	0.0307	0.0715	0.3344	1.32
Nd^{3+}	3	$^4F_{3/2}$	$^4I_{13/2}$	0	0	0.2117	1.35
Dy^{3+}	9	$^6H_{9/2} + ^6F_{11/2}$	$^6H_{15/2}$	0.9394	0.8465	0.4078	1.32

tive transition' [46]. The 615-nm emission of the Eu^{3+} ion, used for red-phosphor, is a typical example, where the $<|U^{(2)}|>^2$ is the largest among the three $<|U^{(t)}|>^2$ [47].

5.2. Spectroscopy of dysprosium in glasses

5.2.1. Judd–Ofelt parameters and optical transitions

Absorption spectra of Dy^{3+} in the fluoride and tellurite glasses are shown in Fig. 13, where the assignment of transitions is also indicated [11]. We can see that the absorption coefficients of transition peaks in this near-infrared region are not so distinct from each other for the fluoride glass. On the other hand, in the tellurite glass the intensity of $^6F_{11/2}+^6H_{9/2}$ band is the largest among all transitions. The Ω_t parameters obtained for the glasses are shown in Fig. 14. The Ω_2 value is the largest in the sulfide and tellurite glasses and decreases in the order $Ga_2S_3 > TeO_2 > ZrF_4 > InF_3$, whereas Ω_6 increases in this order. The change in the absorption cross-section of the $^6F_{11/2}+^6H_{9/2}$ band due to glass compositions can be ascribed to the set of the reduced matrix elements [11]. The $<^6F_{11/2}|U^{(2)}|^6H_{15/2}>^2$ is the largest among three $<|U^{(t)}|>^2$ (t = 2, 4, 6), thus the $S_{JJ'}$ of this band is dependent on the Ω_2 of Dy^{3+} ion in the host. The $<|U^{(2)}|>^2$ of other transitions are small or zero and the $S_{JJ'}$ of them is dependent mainly on Ω_6. It is known that Ω_2 is affected by the local symmetry of ligand field and bond covalency [15]. The electronegativity of the anions is as follows; S < O < F [48]. Therefore, the chemical bond covalency between the Dy^{3+} and the ligand varies with compositions: $Ga_2S_3 > TeO_2 > ZrF_4 > InF_3$. Therefore, the opposite tendency of Ω_2 and Ω_6 against glass compositions can be understood in terms of the differences in the bond covalency in the glasses [37].

Table 3. Lifetime and quantum efficiency of the Dy^{3+} level for 1.3-μm emission in several glass systems.

Host	Lifetime (μs)	Quantum efficiency
Pb–Bi–Ga–O	5	1.5% [53]
Ge–Ga–S	38	17% [12]
Ga–La–S	59	19% [13]
Ge–As–Se	300	90% [49]

5.2.2. Can dysprosium be a candidate?

Because of the large branching ratio and cross section of 1.3 μm, an efficient amplifier can be expected if the nonradiative loss were reduced. Table 3 shows the lifetime and quantum efficiency of Dy^{3+} in several glasses. A selenide glass host can give 90% quantum efficiency [49], which is mainly due to the phonon energy being much smaller than even sulfides. This efficiency seems high enough for practical devices. Moreover, smaller electron-phonon coupling strength in chalcogenides [50] seems more promising for smaller multiphonon loss at levels with a small energy gap than in a host with comparable phonon energy, such as chlorides.

One more problem of Dy^{3+} is bottlenecking at lower levels with longer lifetimes resulting in depression of pumping efficiency and large emission intensities at longer-wavelength side [51], because the energy gap of the lower levels is larger than that of the 1.3-μm level. If the quantum efficiency of the

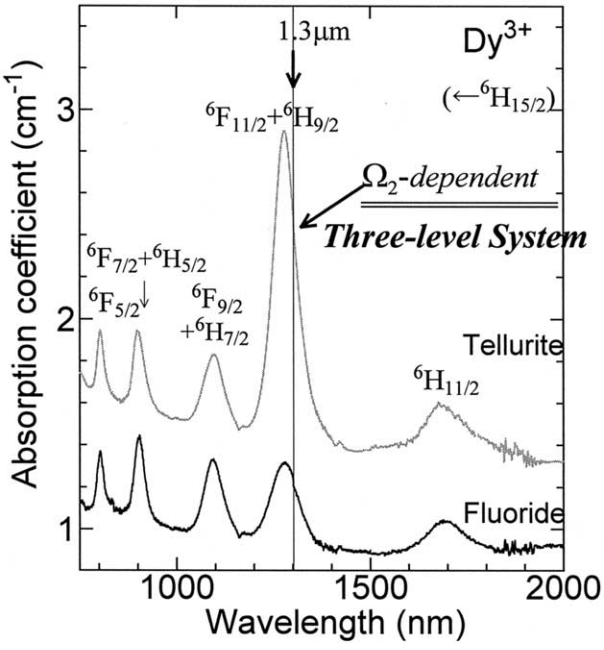

Fig. 13. Absorption spectra of Dy^{3+}-doped glasses.

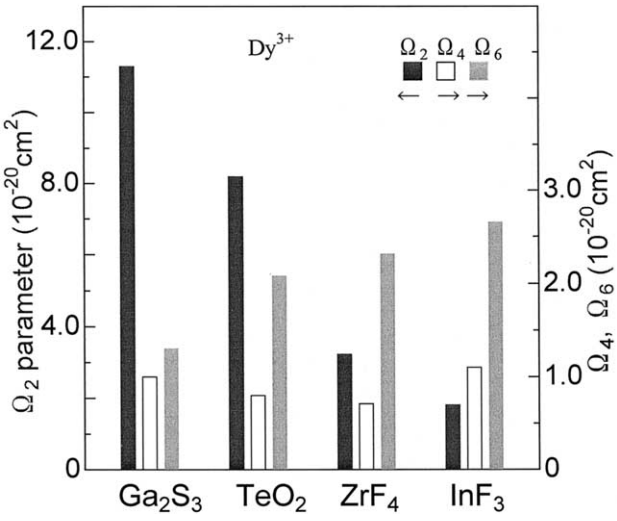

Fig. 14. Ω_t parameters of Dy^{3+} ions in glasses.

1.3-μm level is large enough, the effect of bottlenecking at lower levels would be negligible, since the excited initial state relaxes directly to the ground state due to the branching ratio of more than 90% [52]. There seems a great potential in Dy^{3+}-doped chalcogenides. Further progress in the fabrication of low-loss single-mode fiber is expected.

6. Conclusions

The broad and flat spectral features of Er^{3+}:1.55 μm transition can be obtained in novel glass compositions with a large Ω_6 parameter. The Er^{3+} spectral change is accompanied by compositional evolution of Er–O bond ionicity and local structure.

The Tm^{3+}:1.46 μm transition shows high quantum efficiency in heavy metal oxide glasses due to the larger energy gap of the $^3H_4$ level than the Pr^{3+}:$^1G_4$. Selective quenching of the terminal level is possible in a Ho-codoped system.

New materials are expected for the optical amplifiers in the future WDM network system, to control the 4f transitions of RE ions, which show a variety of spectroscopy in glasses.

References

[1] R.J. Mears, L. Reekie, I.M. Jauncey, D.N. Payne, Tech. Digest OFC/IOOC'87, Reno, Nevada, 1987, p. 167.

[2] C.J. Koestner, E. Snitzer, Appl. Opt. 3 (1964) 1182.

[3] S.B. Poole, D.N. Payne, M.E. Fermann, Electron. Lett. 21 (1985) 737.

[4] E. Snitzer, H. Po, F. Hakimi, R. Tumminelli, B.C. McCollum, Tech. Digest OFC'88, 1988, p. 447.

[5] E. Snitzer, R. Woodcock, Appl. Phys. Lett. 6 (1965) 45.

[6] A. Mori, Y. Ohishi, M. Yamada, H. Ono, Y. Nishida, K. Oikawa, S. Sudo, OFC'97, 1997, PD1.

[7] Y. Ohishi, T. Kanamori, T. Kitagawa, S. Takahashi, E. Snitzer, G.H. Sigel Jr, Opt. Lett. 16 (1991) 1747.

[8] E. Ishikawa, H. Tawarayama, K. Ito, H. Aoki, H. Yanagita, H. Toratani, Tech. Rep. IECIE, 1996 OPE96-111.

[9] K. Wei, D.P. Machewirth, J. Wenzel, E. Snitzer, G.H. Sigel, Opt. Lett. 19 (1994) 904.

[10] D.W. Hewak, B.N. Samson, J.A. Mederios Neto, R.I. Laming, D.N. Payne, Electron. Lett. 30 (1994) 968.

[11] S. Tanabe, T. Hanada, M. Watanabe, T. Hayashi, N. Soga, J. Am. Ceram. Soc. 78 (1995) 2917.

[12] http://www.joho.soumu.go.jp/pressrelease/japanese/tsusin/000615j502.html.

[13] J. Ballato, R. Riman, E. Snitzer, J. Non-Cryst. Solids 213–214 (1997) 126.

[14] S. Tanabe, K. Hirao, N. Soga, J. Non-Cryst. Solids 113 (1989) 178.

[15] S. Tanabe, K. Hirao, N. Soga, J. Non-Cryst. Solids 142 (1992) 148.

[16] S. Tanabe, S. Todoroki, New Glass 7 (1992) 189.

[17] S. Tanabe, K. Suzuki, N. Soga, T. Hanada, J. Lumin. 65 (1995) 247.

[18] C.A. Bracket, J. Lightwave, Technol. 14 (1996) 936.

[19] W.T. Carnal, P.R. Fields, K. Rajnak, J. Chem. Phys. 49 (1968) 4424.

[20] S. Tanabe, T. Hanada, J. Non-Cryst. Solids 196 (1996) 101.

[21] S. Tanabe, T. Ohyagi, S. Todoroki, T. Hanada, N. Soga, J. Appl. Phys. 73 (1993) 8451.

[22] S. Tanabe, T. Hanada, T. Ohyagi, N. Soga, Phys. Rev. B 48 (1993) 10591.

[23] S. Tanabe, S. Yoshii, K. Hirao, N. Soga, Phys. Rev. B 45 (1992) 4620.

[24] B.R. Judd, Phys. Rev. 127 (3) (1962) 750.

[25] G.S. Ofelt, J. Chem. Phys. 37 (3) (1962) 511.

[26] M.J. Weber, Phys. Rev. 157 (1967) 262.

[27] S. Tanabe, T. Ohyagi, N. Soga, T. Hanada, Phys. Rev. B 46 (1992) 3305.

[28] N. Sugimoto, S. Tanabe, S. Ito, T. Hanada, Proc. 10th Meeting Glasses for Photonics, Tokyo, January 1999, p. 32.

[29] H. Taga, Tech. Digest 10th Optical Amplifiers and their Applications, OSA, Washington, DC, June 1999, WC1, 1999, p. 22.

[30] A. Mori, Y. Ohishi, S. Sudo, Electron. Lett. 33 (10) (1997) 863.

[31] J.S. Wang, E.M. Vogel, E. Snitzer, Opt. Mater. 3 (1994) 187.

[32] T. Sakamoto, A. Aozasa, T. Konamori, K. Hoshino, M. Yamada, M. Shimizu, Tech. Digest 10th Optical Amplifiers and their Applications, OSA, Washington DC, June, 1999, WD2-1, p. 50.

[33] R.M. Percival, D. Szebesta, J.R. Williams, Electron. Lett. 30 (13) (1994) 1057.

[34] T. Sakamoto, M. Shimizu, T. Kanamori, Y. Terunuma, Y. Ohishi, M. Yamada, S. Sudo, IEEE Photonics Tech. Lett. 7 (9) (1995) 983.

[35] T. Komukai, T. Yamamoto, T. Sugawa, Y. Miyajima, IEEE J. Quantum Electron. 31 (11) (1995) 1880.

[36] S. Tanabe, K. Suzuki, N. Soga, T. Hanada, J. Opt. Soc. Am. B 11 (5) (1994) 933.

[37] S. Tanabe, K. Tamai, K. Hirao, N. Soga, Phys. Rev. B 53 (13) (1996) 8358.

[38] S. Tanabe, T. Kouda, T. Hanada, Opt. Mater. 12 (1999) 35.

[39] T. Kasamatsu, Y. Yano, H. Sekita, Opt. Lett. 24 (23) (1999) 1684.

[40] P.M. Percival, D. Szebesta, S.T. Davey, Electron. Lett. 29 (12) (1993) 1054.

[41] S. Tanabe, K. Tamai, K. Hirao, N. Soga, Phys. Rev. B 47 (5) (1993) 2507.

[42] S.E. Stokowsky, R.A. Saroyan, M.J. Weber, Nd-doped laser glass spectroscopic and physical properties, Lawrence Libermore National Laboratories, University of California, CA, 1981.

[43] S.G. Grubb, W.L. Barnes, E.R. Taylor, D.N. Payne, Electron. Lett. 26 (1990) 121.

[44] T. Whitley, R. Wyatt, D. Szebesta, S. Davey, J.R. Williams, Tech. Digests OAA'92, Washington, DC, 1992, PD4.

[45] Y. Ohishi, J. Temmyo, Bull. Ceram. Soc. Jpn 28 (1993) 110.

[46] C.K. Jørgensen, B.R. Judd, Mol. Phys. 8 (1964) 281.

[47] M.J. Weber, in: H.M. Crosswhite, H.M. Moos (Eds.), Optical Properties of Ions in Crystals, Wiley-Interscience, New York, USA, 1966, p. 467.

[48] L. Pauling, The Nature of Chemical Bond, 3rd ed., Cornel University Press, Ithaca, New York, 1960, p. 93.

[49] L.B. Shaw, B.J. Cole, J.S. Sanghera, I.D. Aggarwal, D.T. Schaafsma, OFC'98 Tech. Digest, WG8, 1998, p. 141.

[50] S. Tanabe, in: G. Adachi (Ed.), Science of Rare Earths, Kagaku-Dojin Kyoto, 1999, p. 780 (in Japanese).

[51] B.N. Samson, T. Schweitzer, D.W. Hewak, R.I. Laming, Opt. Lett. 22 (1997) 703.

[52] J. Heo, Y.B. Shin, H.-S. Kim, Tech. Digest OFC'99, San Diego, CA, USA, February 1999 #WG7, p. 120.

[53] Y.-G. Choi, J. Heo, J. Non-Cryst. Solids 217 (1997) 199.